Variability of sea ice melt and meteoric water input in the surface Labrador Current off Newfoundland

Marion Benetti, Gilles Reverdin, Catherine Pierre, S. Khatiwala, B. Tournadre, Sólveig R. Ólafsdóttir, Aïcha Naamar

AGU PUBLICATIONS

JGR

Journal of Geophysical Research: Oceans

RESEARCH ARTICLE

10.1002/2015JC011302

Variability of sea ice melt and meteoric water input in the surface Labrador Current off Newfoundland

M. Benetti[1,2], G. Reverdin[1], C. Pierre[1], S. Khatiwala[3], B. Tournadre[1], S. Olafsdottir[4], and A. Naamar[1]

[1]Sorbonne Universités (UPMC, Univ Paris 06)-CNRS-IRD-MNHN, LOCEAN Laboratory, Paris, France, [2]Now at Institute of Earth Sciences, University of Iceland, Reykjavik, Iceland, [3]Department of Earth Sciences, University of Oxford, South Parks Road, Oxford, UK, [4]Marine Research Institute, Reykjavik, Iceland

Key Points:
- The salinity seasonal cycle is explained by the sea ice melt and meteoric water input variability
- The patches of large SIM contribution were located on the continental slope or further offshore
- The data set shows the persistence of sea ice processes during the mid-1990s and 2012–2015

Citation:
Benetti, M., G. Reverdin, C. Pierre, S. Khatiwala, B. Tournadre, S. Olafsdottir, and A. Naamar (2016), Variability of sea ice melt and meteoric water input in the surface Labrador Current off Newfoundland, *J. Geophys. Res. Oceans*, *121*, 2841–2855, doi:10.1002/2015JC011302.

Received 5 SEP 2015
Accepted 9 MAR 2016
Accepted article online 14 MAR 2016
Published online 26 APR 2016

Abstract The respective contributions of saline (Atlantic and Pacific water) and freshwater (sea ice melt, meteoric water) components in the surface Labrador Current are quantified using salinity, $\delta^{18}O$, and nutrient data collected between 2012 and 2015 east of Newfoundland to investigate the seasonal variability of salinity in relation with the different freshwater contributions. Nutrient data indicate that the surface saline water is composed on average over 2012–2015 of roughly 62% Atlantic Water and 38% Pacific Water. A large salinity seasonal cycle of $\approx$ 1.5 peak-to-peak amplitude is found over the middle continental shelf, which is explained by the freshwater input seasonal variability: 2/3 of the amplitude of the salinity seasonal cycle can be explained by meteoric water input and 1/3 by the sea ice melt. A smaller seasonal salinity cycle ($\approx$1.3) is observed over the inner shelf compared to the middle shelf, because of smaller variability in the large meteoric water inputs. Furthermore, the data reveal that sea ice melt (SIM) input was particularly important during July 2014, following a larger extension of sea ice over the Labrador shelf during the 2013/2014 winter season, compared to both previous winter seasons. Some patches of large SIM contribution observed during July 2014 and April 2015 were located on the continental slope or further offshore. The comparison of 2012–2015 data with data collected in 1994–1995 shows that the surface water over the Newfoundland shelf and slope is strongly affected by sea ice processes in both periods and suggests a larger contribution of brines over the slope during 1994–1995.

1. Introduction

The surface North Atlantic subpolar gyre (SPG) presents a cyclonic circulation (Figure 1), where warm and salty water originating from the subtropical gyre meets fresh and cold water from the Arctic regions. Deep convection can reach 2000 m depth within the gyre [*Lazier*, 1973; *Rhein et al*., 2002; *Yashayaev and Loder*, 2009] and transforms the surface water into intermediate water, an important step in the meridional overturning circulation (MOC). This water mass transformation is strongly influenced by surface salinity and temperature [*Lazier*, 1973; other studies as *Latif et al*., 2006]. Several studies have shown that the surface salinity of the SPG evolves on seasonal to interdecadal time-scales [*Belkin*, 2004; *Reverdin et al*., 2003; *Reverdin*, 2010]. This variability can be due to the variable input of salty and warm waters from the subtropical gyre [*Desbruyères et al*., 2015] or of fresh and cold waters from the Arctic regions [*Dickson et al*., 1988; *Yashayaev et al*., 2007]. This study focuses on inputs of freshwater from high latitudes and more specifically, on the Labrador Current (LC), which carries a significant amount of Arctic-origin freshwaters to lower latitudes [*Mertz et al*., 1993], either directly from the Canadian Arctic, or indirectly via the west and east Greenland Current systems. It exchanges with the interior SPG, where most of its water ultimately enters. For example, *Fratantoni and McCartney* [2010] show that large amounts of freshwater from the LC are advected offshore at Flemish Cap (near 48°N).

The surface circulation of the northern North Atlantic (NNA) is schematically shown in Figure 1. The fresher and colder waters from the Arctic are carried into the SPG by three main currents: the East Greenland Current (EGC), the West Greenland Current (WGC), and the LC. The EGC carries fresh and cold water across Fram Strait along the eastern coast of Greenland. The WGC is an extension of the EGC and flows north along the west Greenland coast. Around 63°N, the WGC separates into two branches. One branch continues further north into Baffin Bay. The other one crosses the Labrador Sea to feed the LC. The LC is an extension of

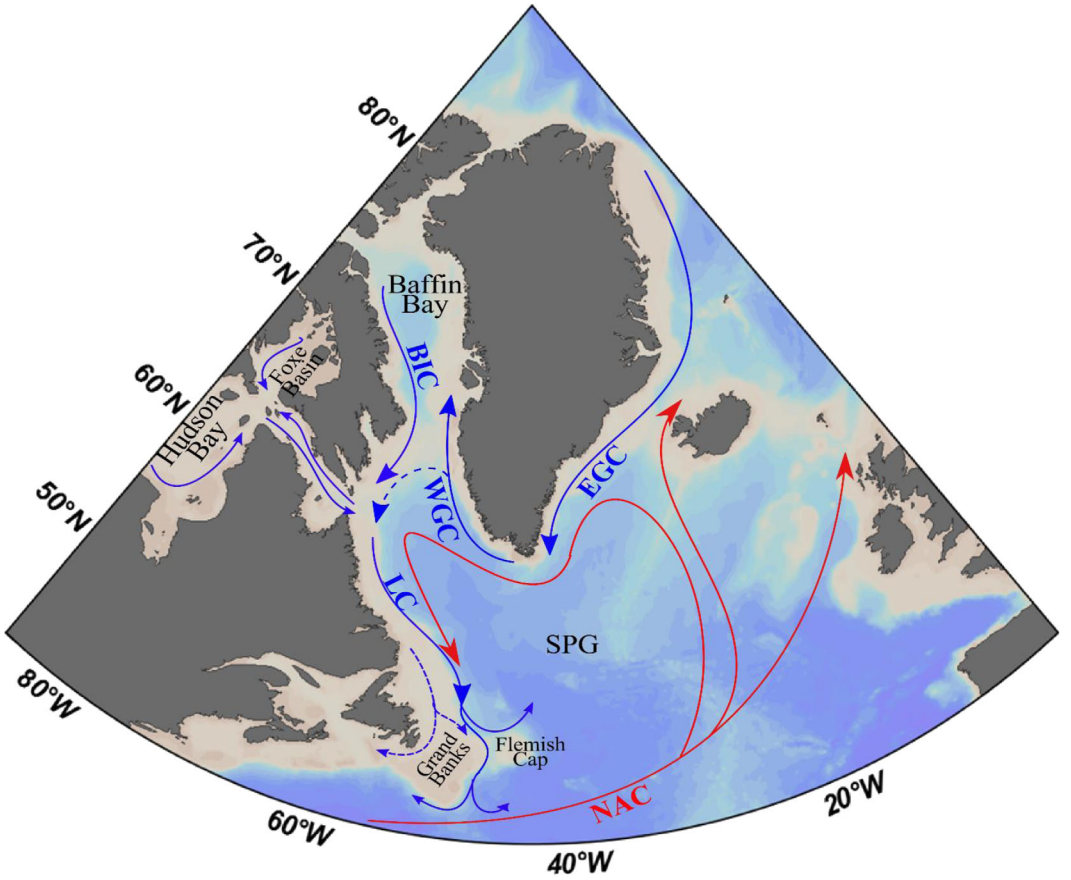

Figure 1. Schematic surface circulation in the Northern North Atlantic. Blue arrows are for cold and fresh currents; red arrow for warm and saline currents. NAC: North Atlantic Current. EGC: East Greenland Current. WGC: West Greenland Current. BIC: Baffin Island Current. LC: Labrador Current. NF: Newfoundland. FC: Flemish Cap. SPG: Subpolar gyre.

both the WGC and the Baffin Island Current (BIC), and also contains the outflow from Hudson Strait. The surface LC flows southeastward over the Labrador shelf and upper slope where it meets warmer waters (often offshore or just below) [*Lazier and Wright*, 1993; *Loder et al*., 1998]. Near Newfoundland, the LC is composed of two branches: an inshore coastal branch (dotted line in Figure 1) and a stronger offshore branch. The inshore branch flows southward near Newfoundland's east coast, and a part turns to the west around the southeastern-most point of Newfoundland.

The LC freshwater budget is in part controlled by (1) the outflow from Hudson Strait and Davis Strait (contributions of Arctic freshwater crossing the Canadian Arctic Archipelago and local freshwater input within Baffin Bay and Hudson Bay), (2) the freshwater components of the EGC/WGC (contributions of Arctic freshwater crossing the Fram Strait and additional freshwater inputs along the Greenland coast) and, (3) local inputs along the Labrador coast inducing excess precipitation over evaporation (P-E) by river runoff and sea-ice melt [e.g., *Mertz et al*., 1993; *Lazier and Wright*, 1993; *Straneo and Saucier*, 2008; *Khatiwala et al*., 1999]. Thus, the LC provides useful information on the exchanges between the Arctic Ocean and the SPG as it contains freshwater exported from the Canadian Arctic Archipelago as well as from the EGC. However, its investigation is complicated by numerous local sources and sinks of freshwater such as sea ice melt, brines associated with ice formation, runoff, precipitation, or continental ice cap melt. How these freshwater sources are redistributed to the SPG through the LC and what their variability is remains poorly known.

Myers et al. [1990] showed that sea ice processes over the northern Newfoundland shelf affect the salinity variability in the inner part of the LC and that changes in exchanges with the Arctic regions could influence LC properties. In addition, the observed increase of the Greenland and Canadian Arctic ice-sheet melt over the period 2000–2012 could also have impacted the LC surface salinity [e.g., *Shepherd et al*., 2012]. In this study, we present a new data set of geochemical tracers to obtain a better understanding of the hydrological processes affecting the surface LC salinity.

We focus on the southern part of the LC off the Newfoundland (NF) coast. First, we establish the seasonal variability of salinity at the surface LC. Then, we use nutrients and oxygen stable isotopes of sea water to estimate the relative contribution of Pacific water (PW), sea ice melt (SIM), and meteoric water (MW) into the LC. The term MW represents precipitation (rain and snow) over the ocean, river runoff, and continental ice cap melt. These data are used to discuss the seasonal and interannual variability of the different freshwater sources of the LC during the period 2012–2015. A comparison is also done with isotopic data collected during the mid-1990s in the same region.

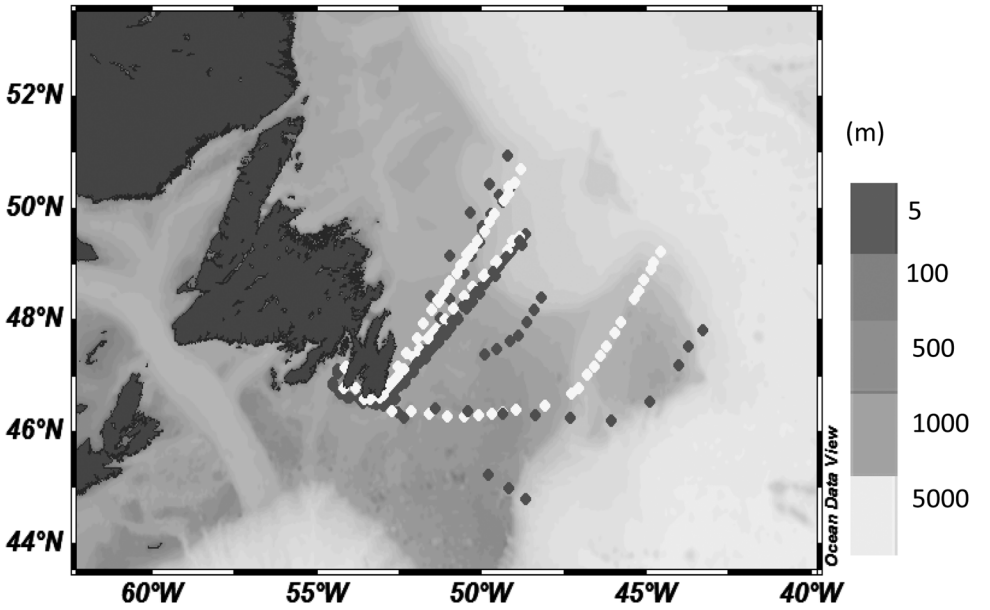

Figure 2. Isotopic sampling of the LC in 1994–2015 period (SURATLANT surface measurements on the Labrador shelf and slope). White points correspond to 1994–1995 cruises and grey points correspond to 2012–2015 cruises. Shading according to bathymetry (darker on shelf). The most southern transect corresponds to the April 2014 SURATLANT cruise. Samples located south of Flemish Cap correspond to the April 2015 SURATLANT cruise.

2. Material and Methods

2.1. Sampling Strategy

Through the SURATLANT project initiated in 1993, surface sampling off the Newfoundland coast was collected from merchant vessels measuring at least salinity, and since 2001 nutrients (dissolved nitrate, phosphate, silicate). Surface water samples for oxygen isotope analysis were also collected every 3 months during two periods: from June 1994 to June 1995 and from March 2012 to June 2015. The positions of the isotope measurements used in this study are shown on Figure 2. In addition, surface salinity measurements are also available on the Newfoundland shelf and slope from the same merchant vessels (typically 20 crossings each year averaged over a 20 year period).

2.2. Sea Surface Salinity

Sea surface salinity (SSS) was continuously measured at ~4–5 m depth (depending on the vessel) by a Thermo-salinograph (TSG seabird Electronics, Inc. USA, model 21) installed on the ship. The SSS was regularly calibrated by conductivity measurements of discrete samples. SSS accuracies were generally estimated at 0.01 during the cruises with surface sampling, but could be less accurate (0.05) at other times.

2.3. Oxygen Isotopes of Sea Water

Since 2012, the oxygen isotopic composition of discrete sea water samples has been analyzed with a PICARRO CRDS (cavity ring-down spectrometer; model L2130-I Isotopic H_2O) at LOCEAN-IPSL (Paris, France). Based on repeated analyses of an internal laboratory standard over several months, the accuracy of the $\delta^{18}O$ measurements was $\pm 0.05‰$. The analyses were performed by running six injections per sample. The first three injections were ignored to eliminate potential memory effects between samples. The remaining three injections were averaged and calibrated against the internal water references. Three internal references which have been used to calibrate the data in the V-SMOW scale ($\delta^{18}O$: $-0.05‰$, $-3.26‰$, $-6.61‰$). All reference waters were stored in steel bottles with a slight overpressure of dry nitrogen to avoid evaporation and exchange with ambient air humidity. These references have been calibrated using IAEA references (GISP and SMOW) and several internal standards from other laboratories have been used to confirm these calibrations. All sea water samples have been distilled to avoid salt accumulation in the vaporizer of the PICARRO system and its potential effect on the measurements [e.g., *Skrzypek and Ford*, 2014]. Two tests were performed in our laboratory to confirm that this operation does not affect the isotopic composition of sea

water (results not shown here). The first one consisted in comparing the isotopic composition of a salty sea water sample with the subsequent distilled sample. The second test consisted in distilling several samples of the same water and to compare the isotopic composition of the distilled samples. Both tests indicated that the distillation process has little impact on the measurement (less than the uncertainties due to the PICARRO measurement).

The $\delta^{18}O$ values of samples of the mid-1990s cruises were analyzed at the Lamont Doherty Earth Observatory on a GV Instruments Isoprime dual inlet IRMS coupled with Aquaprep sample preparation system. Contrary to cavity ring down spectrometer, these analyses were performed by equilibrating the sea water sample with a reference CO_2 gas of known $\delta^{18}O$ value. Because the method of measurement differs between the two periods, we have duplicated and compared freshwater and sea water measurements done on the PICARRO L2130i at LOCEAN with (1) laboratories using mass spectrometers coupled with Aquaprep sample preparation system (IRMS-Aquaprep) (same spectrometer as one used in the mid-1990s at LDEO) and (2) laboratories using laser spectrometry (LS) (same spectrometer as at the LOCEAN). The results are presented in Appendix A. Briefly, the comparisons show that all measurements (freshwater) done with LS are consistent, which confirms the expected accuracy of measurements done at the LOCEAN. Unfortunately, no comparison with sea water has been done because the laboratories taking part to this project did not measure sea water with their LS. However, both tests presented previously indicate that freshwater and sea water measurements done with the LS at LOCEAN are consistent. The comparisons with IRMS-Aquaprep show an offset of approximatively $+0.14‰$ for sea-water measurements compared to LS measurements (no offset observed for freshwater measurements). An offset of $+0.15‰$ between saline water with salinity around $35‰$ and freshwater measured with IRMS-Aquaprep was also observed by *Lécuyer et al*. [2009]. Although the origin of this offset is still not fully understood, we decided to apply a correction of $-0.15‰$ to the mid-1990s $\delta^{18}O$ measurements done with a IRMS-Aquaprep to compare them with the 2012–2015 measurements done with the LS. Unfortunately, we did not have the possibility to do a more direct intercomparison between the two laboratories as the IRMS-Aquaprep formerly used at LDEO is now out-of-service.

2.4. Nutrients

Dissolved inorganic nutrient data have been collected during all 2012–2015 cruises and measured with standard colorimetric methods at the Marine Research Institute (Reykjavik, Iceland). The analytical procedure and the quality control for the nutrient analyses have been described in detail in *Olafsson et al*. [2010], where the long-term accuracy was estimated as ± 0.2 μmol.L^{-1} for nitrate and ± 0.03 μmol.L^{-1} for phosphate, the two inorganic nutrients we consider in the study.

3. Calculation of the Freshwater Contributions and Uncertainties

We separate the mass contributions to the LC in sea ice melt (SIM), meteoric water (MW), and saline sea water inputs. We consider two types of sea water affecting the surface LC: Atlantic water (AW), which is the main sea water influencing the region, and Pacific water (PW), which comes from Bering Strait, crosses in the Arctic Ocean and reaches the LC mainly through the Davis Strait. The first step is to estimate the relative proportions of AW (f_{AW}) and PW (f_{PW}) in the LC, and thus the salinity and $\delta^{18}O$ of the saline water affecting the LC (e.g., $S_{seawater} = f_{AW}S_{AW} + f_{PW}S_{PW}$). Then, the contribution of SIM (f_{SIM}) and MW (f_{MW}) to the LC surface water can be determined for each sample by using measured salinity and $\delta^{18}O$. In the following, we present the mass balance calculations used to estimate the contributions of each water source into the LC. Then, we define the characteristics (nutrients, $\delta^{18}O$, and salinity) of each end-member affecting the system. Finally, we discuss the uncertainties of the method.

3.1. Calculation of AW and PW Fraction

AW and PW are transported into the LC, which receives Arctic waters from Fram and Davis Straits. Using the approach of *Jones et al*. [1998, 2008], we used dissolved nitrate and phosphate concentrations to estimate the contributions of PW and AW [e.g., *Yamamoto-Kawai et al*., 2008; *Sutherland et al*., 2009; *Bauch et al*., 2011; *Dodd et al*., 2012]. The different nitrate-phosphate relationships proposed to characterize PW and AW are shown on Figure 3. The principle is briefly summarized as follows. In the global ocean, the N:P ratio is usually around 16 and can be approximated as constant during biological production and regeneration of

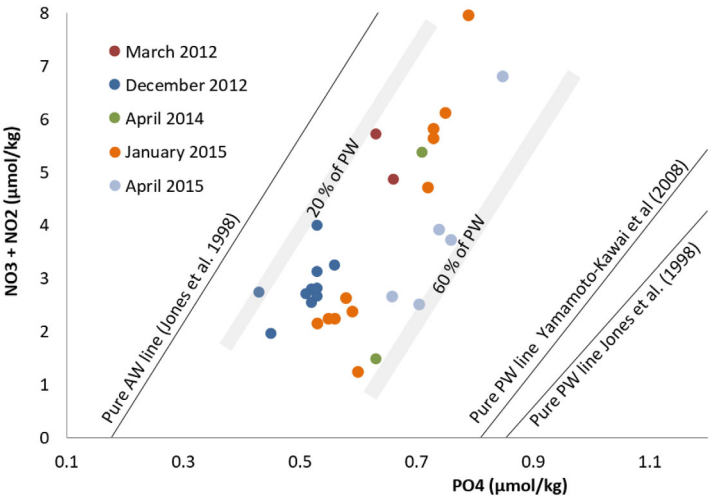

Figure 3. Scatter diagram of nitrate versus phosphate concentrations. Black solid lines show reported N/P relationships for AW and PW from literature. Colored dots are shelf surface samples in winter and early spring between 2012 and 2015. The PW "boundary" fractions surrounding the samples (20% and 60%) are derived from equation (1), and shown on the diagram. Considering all the shelf samples, the mean value of f_{PW} is estimated as 0.38 ± 0.12% (0.40 ± 0.12% using the N/P relationship of *Yamamoto-Kawai et al.* [2008] for PW).

organic matter [*Redfield*, 1958, 1963; *Falkowski and Davis*, 2004; *Arrigo*, 2005]. However, PW entering the Arctic Ocean across the Bering Strait is depleted in nitrate relative to phosphate compared to AW [*Jones et al.*, 2008; *Yamamoto-Kawai et al.*, 2008]. This depletion is due to denitrification processes occurring over the sediments on the Bering and Chuckchi shelves [*Cooper et al.*, 1997; *Jones et al.*, 1998].

The fraction of PW is calculated as follows [e.g., *Sutherland et al.*, 2009]

$$f_{pw} = \frac{N^m - N^{AW}}{N^{PW} - N^{AW}} \quad (1)$$

where N total nitrate is the sum of nitrate and nitrite. N^m is the measured total nitrate value, N^{AW} and N^{PW} are respectively the total nitrate value for pure Atlantic and Pacific water. N^{AW} and N^{PW} values are calculated by substituting the PO_4^m value in the equation of the pure AW and PW line. Note that SIM and MW contributions are assumed to have the nutrients in the same proportion as the AW.

3.2. Calculation of SIM and MW Fraction

Once the ratio of PW and AW proportions has been established, we use the $\delta^{18}O$-salinity relationship to discriminate the SIM and MW contributions [e.g., *Craig and Gordon* 1965; *Östlund and Hut*, 1984; *Melling and Moore*, 1995]. Because $\delta^{18}O$ of sea-ice melt is high compared to $\delta^{18}O$ of MW and both sources have very low salinity, the $\delta^{18}O$-S relationship is particularly useful to discriminate the influence of SIM and of MW on LC surface salinity. This means that water resulting from dilution of sea water with SIM (MW) lies on a line with a low (high) slope. An intermediate slope is found if both processes are present and all the sources are mixed. The fractions of the freshwater sources can also be determined following the method of *Östlund and Hut* [1984]. The mass balance calculations are presented below:

$$f_{AW} + f_{PW} + f_{MW} + f_{SIM} = 1 \quad (2)$$

$$f_{AW} \cdot S_{AW} + f_{PW} \cdot S_{PW} + f_{MW} \cdot S_{MW} + f_{SIM} \cdot S_{SIM} = S_m \quad (3)$$

$$f_{AW} \cdot \delta O^{18}_{AW} + f_{PW} \cdot \delta O^{18}_{PW} + f_{MW} \cdot \delta O^{18}_{MW} + f_{SIM} \cdot \delta O^{18}_{SIM} = \delta O^{18}_m \quad (4)$$

where S_m and δO^{18}_m are the measured values. f_{AW}, f_{PW}, f_{MW}, f_{SIM} are the relative fraction of AW, PW, MW, and SIM. Equation (3) is for the mass conservation of salinity and equation (4) is for the conservation of $\delta^{18}O$. A negative f_{SIM} indicates net formation of sea ice, while a positive fraction indicates net melting of sea ice.

3.3. End-Members and Uncertainties of the Method

The calculations presented above require knowledge of the properties of each water mass source. The uncertainties on these end-member properties are the main limitations of the fraction calculations and require sensitivity tests. These issues are briefly summarized in this section and are discussed in more detail in Appendix B, which presents the sensitivity tests.

3.3.1. Nutrient Properties of AW and PW

With respect to the f_{AW} and f_{PW} estimations, the error is mostly related to the definition of the AW and PW nutrient properties, and neglecting biogeochemical processes that would cause deviations in standard

Table 1. Salinity and $\delta^{18}O$ Characteristics of the End-Members Used in the Mass Balance Calculations

Water Mass	S (Mean Value)	$\delta^{18}O$ (Mean Value in ‰)	References
Atlantic water	35	+0.18	This study (Appendix B)
Pacific water	32.5	−1	*Cooper et al.* [1997] Woodgate and Aagaard [2005]
Meteoric water	0	−18.4	*Cooper et al.* [2008]
Sea ice melt	4	+0.5	*Melling and Moore* [1995] *Östlund and Hut* [1984]

stoichiometric ratios of dissolved inorganic N/P. Recent studies [*Bauch et al*., 2011; *Yamamoto-Kawai et al*., 2008] showed that the relationship between N/P in PW as estimated by *Jones et al*. [1998] could induce errors on estimated PW fraction by two different mechanisms: (1) further denitrification can occur within the bottom sediment on the Laptev and Barents Sea shelves and (2) nitrification can occur in cold shelf waters where ammonium content is high. Unfortunately, we did not measure the ammonium content. The N/P relationship in PW estimated by *Yamamoto-Kawai et al*. [2008], which takes into account the ammonium content, is shown as well as the one from *Jones et al*. [1998] on Figure 3. Assuming the pure Atlantic and Pacific lines are parallel, the relative distance of any point from the two lines indicates the relative proportions between PW and AW. In our case, the difference between the two PW lines does not significantly change the calculation of PW and AW fractions (by approximatively 2%). Altogether, authors using similar methods considered an uncertainty of 10–14% on the estimation of the AW and PW fractions [*Jones et al*., 1998; *Sutherland et al*., 2009; *Dodd et al*., 2012; *Bauch et al*., 2011; *Taylor et al*., 2003].

3.3.2. Salinity and $\delta^{18}O$ Properties of the End-Members

The salinity and $\delta^{18}O$ values of each end-member used in the calculations are presented in Table 1. Their possible ranges of variations are discussed in Appendix B.

The salinity and $\delta^{18}O$ of the PW have been set following the approach of *Dodd et al*. [2012]. We used a salinity of 32.5 ± 0.3 (flow weighted mean salinity calculated by *Woodgate and Aagaard* [2005]) and $\delta^{18}O = -1 \pm 0.2‰$. The $\delta^{18}O$ value is determined from the relationship between S and $\delta^{18}O$ measured by *Cooper et al*. [1997] on the Bering Sea shelf.

The salinity and $\delta^{18}O$ of the AW have been estimated from the SURATLANT cruise, which also sampled the region south of Iceland, largely affected by the AW carried along the Irminger Current. We consider that the salinity 35 characterizes AW and we found consistent measured values of $\delta^{18}O = +0.18 \pm 0.05‰$ for this salinity during all the cruises between 2012 and 2015 (see the measurements in Appendix B).

Melling and Moore [1995] measured salinity of growing first-year sea ice in the Beaufort Sea in March 1987 varying from 4.44 to 7.73, but measurements of sea-ice salinity are too rare to use an averaged salinity from this sampling. As a result, we use a mean salinity of ice equal to 4 as done in the study of *Östlund and Hut* [1984].

To estimate the $\delta^{18}O$ of the sea ice, we use the fractionation factor established from several observations in the Beaufort Sea by *Melling and Moore* [1995]. They found that sea ice is enriched by +2.1‰ compared to the sea water source. We apply this isotopic fractionation between liquid and solid on the mean $\delta^{18}O$ value of the Arctic Ocean estimated at −1.57‰ [*Melling and Moore*, 1995; *Östlund and Hut*, 1984]. Thus, we use a value of +0.5‰ for sea ice melt.

Larger uncertainties exist in the $\delta^{18}O$ value of the MW, in part because rain and snow measurements during the full year over the Arctic Ocean are rare due to the difficulties of sampling. Moreover, in the region we consider, MW also contains continental ice cap melt and snow melt with considerable spatial and interannual variations, so that an overall synthesis is not possible. Here, we chose $\delta^{18}O = -18.4‰$, but test the sensitivity of our results with values from −16 to −23‰. This point is discussed in detail in Appendix B.

3.3.3. Discussion of the Uncertainties

Sensitivity tests to the variability of the end-member properties ($\delta^{18}O$, S, f_{PW}) are presented in the Appendix B and show that the largest uncertainties of this method reside in the choice of PW properties, MW $\delta^{18}O$ value and PW:AW ratio. These variations are conceivable and could have an effect on the order of 1% on the MW and SIM fractions. Most commonly, other similar studies have suggested uncertainties of 1–2%, in agreement with our sensitivity tests.

4. Results

4.1. Mean Contribution of PW and AW in the Surface LC Over 2012–2015

The PW:AW ratio in waters flowing through the Canadian Arctic Archipelago into the BIC and then the LC, but also from the west Greenland Current can evolve with the atmospheric forcing variability affecting the Arctic region (e.g., NAO/AO phase, position of the transpolar drift) [*Sutherland et al*., 2009; *Lique et al*., 2010]. In this section, we estimated the PW:AW ratio in the surface LC from the SURATLANT cruises between 2012 and 2015. During the summer cruises, the nutrient contents were strongly modified over the surface Newfoundland shelf (to the point where N was depleted to zero). We found from other measurements (0–300 m) in the Labrador current (around 52–54°N) (not shown here) that biological processes affected phosphates in the nitrate-depleted surface layer over the Labrador shelf and lead to unusually low values of PW fractions. Thus, we preferred in this study to use only winter cruises to limit errors in the PW fraction calculation. Assuming a weak seasonal variation in the relative proportions of AW and PW (based only on December–April measurements, see Figure 3), we extrapolated the proportions found in winter to the summer measurements. The shelf samples corresponding to the LC are shown in Figure 3 and indicate a mean proportion of approximately $38 \pm 12\%$ PW affecting the surface LC during 2012–2015 (the PW fractions are derived from equation (1), using the N/P relationships of *Jones et al*. [1998]). Furthermore, nutrient winter data on the surface Newfoundland shelf from 2001 to 2010 (not shown) revealed the same magnitude for the PW fraction in the surface LC. Nonetheless, Figure 3 also suggests interannual variability with more contribution of PW during the winters 2014–2015 compared to 2012. The interannual variability of PW fractions in the east Greenland Current have been investigated by *Rabe et al*. [2013] and *De Steur et al*. [2015] who suggested a recent larger amount of the PW fraction compared to the previous decade. In particular, the Pacific water influence in Fram Strait increased between 2010 and 2011 [*Rabe et al*., 2013], and is seen as larger values in 2013 in Denmark Strait. To our knowledge, no such records are published for the Labrador Current. As we do not have nutrient measurements for each $\delta^{18}O$ water sample, we decided to apply a constant proportion of 38% for PW and 62% for AW to define the saline water component influencing the surface Newfoundland shelf (without considering the possible interannual and seasonal variability). In Appendix B, we tested the effect of a 20% variation of PW fraction, corresponding to the potential interannual variability we observe in the data. This variability has no effect on the SIM fraction but an effect of 1% on the MW fraction.

4.2. Seasonal Variability of the Freshwater Input to the Surface LC (2012–2015)

4.2.1. The Salinity Seasonal Cycle at the Surface LC

Salinity measurements from the regular sampling on the Newfoundland shelf (typically 20 crossings each year averaged over a 20 year period to reduce sampling uncertainties) are combined to estimate the surface salinity cycle of the LC across the Newfoundland shelf (Figure 4). On the inner shelf, the range of seasonal variability of salinity was around 1.3 with a maximum in April and a minimum in September. This salinity seasonal cycle has a similar magnitude as the one observed during 40 years at station 27 (0–30 m) close to the Newfoundland coast (decrease of 1.2 between March and September/October [*Myers et al*., 1990]). On the middle-shelf, we found a slightly stronger seasonal cycle with an amplitude around 1.5, with a maximum in March/April and a minimum in September. On the continental slope, the amplitude was around 0.9 with a maximum in February and a minimum in August. Further offshore, after the surface isohaline 34, the salinity seasonal cycle was weaker and decreased quickly when the cold and fresh waters of the LC met the relatively warm and salty waters of the interior gyre.

4.2.2. Seasonal Variations of SIM and MW Input at the Surface LC

In this section, we will address how the sea-ice processes and the meteoric water inputs contribute to the salinity seasonal variations at the surface LC. Figure 5 presents the winter (from the end of December to the start of April, green) and summer data (from the end of June to the start of October, red) in the $\delta^{18}O$-S diagram. The samples with salinity ranging between 34 and 34.6 were located further toward the interior of the gyre and were less influenced by the freshwater input from the LC. The samples with lower salinity (<34) represent the LC along the slope as well as the shelf waters. Figure 5 reveals different $\delta^{18}O$-S relationships as a function of the season. The linear regressions were $\delta^{18}O = 0.55 \pm 0.25 \times S - 18.93 \pm 0.80$ for summer cruises and $\delta^{18}O = 0.67 \pm 0.25 \times S - 22.53 \pm 0.77$ for winter cruises. This $\delta^{18}O$-S distribution suggests that surface salinity both on shelf and slope was seasonally influenced by sea ice melt/formation (see the grey arrow in Figure 5, when sea ice is melting, the salinity of the surrounding sea water strongly

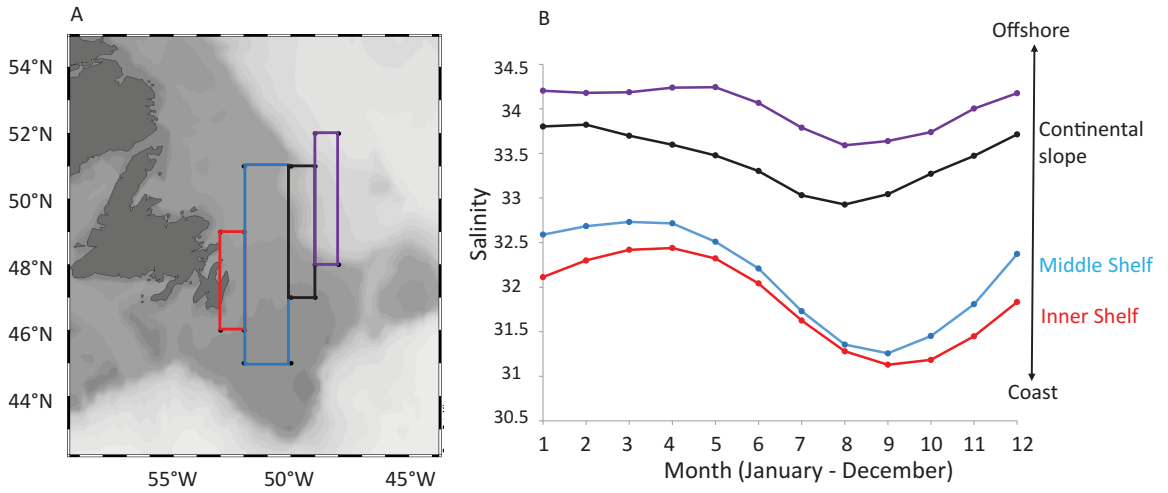

Figure 4. (a) Boxes for which an average seasonal cycle was derived. The red area corresponds to the inner shelf, the blue area to the middle shelf and the black, and the purple areas to the continental slope. (b) The seasonal surface salinity cycle over the Newfoundland shelf and slope (typically 20 crossings each year averaged over a 20 year period). Each point corresponds to the average monthly value.

decreases compared to the isotopic composition). The *y* intercept of $-22.53‰$ (lower than the mean $\delta^{18}O$ value of MW, $-18.4‰$) indicates the influence of brine formation at the surface LC in winter. Note that the sea ice influence was much weaker than what was observed further north (e.g., Fram Strait) [*Dodd et al.*, 2012] where sea ice formation was considerably more important, leading to much lower value of the *y* - intercept. Over the continental shelf, the $\delta^{18}O$-S relationship indicates that about 0.5 of the salinity seasonal cycle amplitude is explained by the sea ice cycle (for a similar $\delta^{18}O$ value, salinity can change by 0.5). Mass balance calculations (equations (2), (3), and (4)) indicate that sea ice melt fractions increased on average by 2% between winter and summer. With the limited sampling, we observe no significant difference in the f_{SIM} spatial variability between the inner and middle shelf (Figure 4 shows the selected areas which characterize the inner and middle shelf in this study).

The amplitude of the salinity cycle over the shelf was higher (1.3 for the inner part −1.5 for the middle part) than the amount of variability attributed to the sea ice cycle (0.5) and must therefore result from a

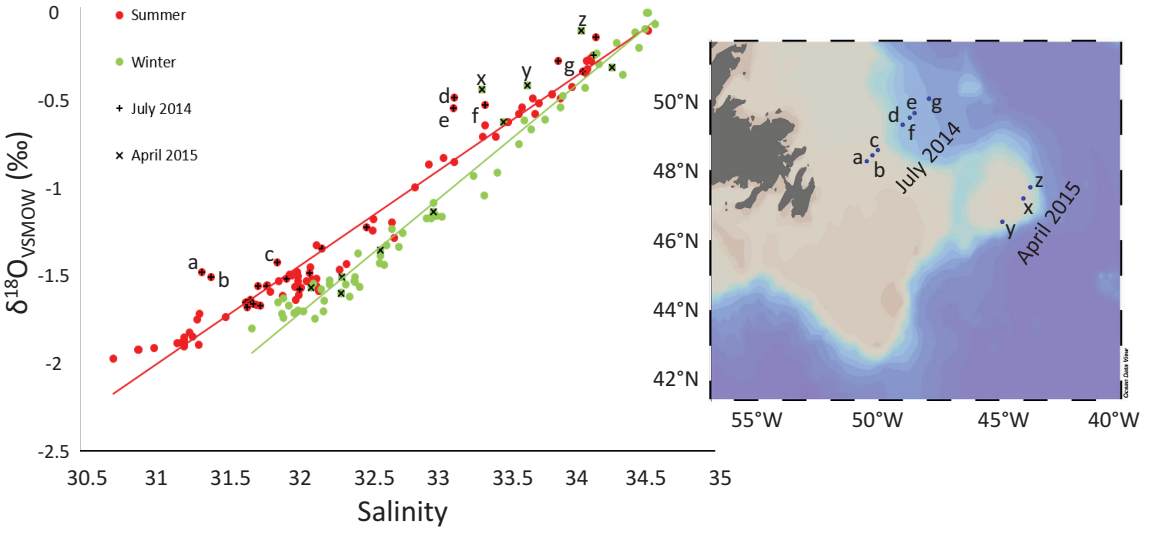

Figure 5. The $\delta^{18}O$-S diagram for winter (from the end of December to the start of April, green) and summer (from the end of June to the start of October, red) cruises between March 2012 and June 2015. The black crosses indicate samples from July 2014 and April 2015. The linear regression is $\delta^{18}O = 0.55 \pm 0.25 \times S - 18.93 \pm 0.80$ ($R = 0.96$) for summer cruises (red) and $\delta^{18}O = 0.67 \pm 0.25 \times S - 22.53 \pm 0.77$ ($R = 0.98$) for winter cruises (green). The samples from July 2014 and April 2015 with particularly high SIM fractions are identified on the map.

Table 2. Fractions of the MW Input (%) Over the Inner and the Middle Shelf in Function of the Season[a]

Month	Inner Shelf	Middle Shelf
Mar	8%	5–6%
Jul	8%	8%
Oct	10%	10%

[a]Figure 4 shows the selected areas which characterize the inner and middle shelf in this study.

combination of SIM and MW exports. How does MW input to the LC evolve and affect the salinity cycle? The low salinity of the LC is largely explained by the important input of surface MW from the Arctic region (as well as river freshwater and ice sheet melt from Greenland and Canadian Arctic). For the whole year, the LC is fresh compared to the SPG. In March, fractions of MW are larger than 5% over the continental shelf and can reach 8% on the inner interior shelf. At the end of summer, these fractions increase to between 9 and 10% on the whole NF shelf. Thus, while a strong input of MW is observed in the LC through the whole year, a difference is observed between March and October leading to seasonal variations of the MW content in the LC. Combining this difference of approximatively 4% in the MW fractions over the middle shelf and around 2% in the sea ice melt fraction between winter and the end of summer is sufficient to explain the full salinity cycle measured on the middle shelf. In short, 2/3 of the amplitude of the surface salinity seasonal cycle over the NF middle shelf can be explained by the MW input variability and 1/3 by the SIM seasonal variability.

As seen previously in Figure 4, the salinity seasonal cycle is slightly smaller over the inner continental shelf compared to the middle shelf. To understand this feature, we investigate the spatial distribution of the MW and its control on the seasonal salinity cycle over the shelf. The averages of the MW fractions in function of the season and of the location on the shelf are presented in Table 2. In the inner part of the LC (around the southeastern-most point of Newfoundland), the fraction of MW mean value was 8% from March to the end of July and was 10% at the end of summer. Thus, there was only 2% increase in the MW fractions between March and the end of summer. There, the MW fraction was high during the whole year, even in late winter. On the middle shelf, the fraction of MW mean values varied between 5 and 6% in March, 8% in early summer, and 10% at the end of summer. Thus, on the middle shelf there was a larger difference between March and the June–July period compared to what was found on the inner shelf. These observations could explain why the amplitude of the salinity seasonal cycle was stronger in the middle shelf than in the inner shelf. Indeed, on the inner shelf, even in March, the fraction of MW stayed relatively important, revealing that the water of the inner part of the shelf was strongly influenced by MW input during most of the year. While it is difficult to do more precise calculations with this present sampling, the previous observations suggest that the salinity seasonal cycle on the inner shelf is explained in equal proportions by the SIM and MW seasonal variability.

4.3. Interannual Variability During 2012–2015 and Comparison With the Mid-1990s

The SURATLANT cruises in 2012–2015 provided a better understanding of the seasonal surface salinity variability over the surface NF shelf. In addition, another aim was to investigate the interannual variability of the SIM and MW input to the surface LC. Thus, this section is a preliminary approach of a long-term survey of the LC variability.

4.3.1. Variability During the 2012–2015 Period

An interesting feature occurred in the Labrador Current during the summer 2014 (late July 2014). The corresponding samples are marked with a black cross in the δ^{18}O-S relationship in Figure 5. Some of these samples are shifted to lower salinities with relatively high δ^{18}O values and reveal a stronger input of sea ice melt in the surface waters compared to samples during the summers 2012 and 2013 (whereas the corresponding MW fractions are rather similar during the different summer cruises). Their locations are shown in Figure 5 and their MW and SIM fractions are presented in Table 3. This stronger influence of sea ice melt at the surface LC followed a particularly large extension of sea ice cover over the Labrador shelf during the winter 2014, in comparison with the earlier winters 2012 and 2013. Note that in March 2012, the sea ice extent was also large but only in the north of the Labrador Sea (observations from NSIDC from January to March). It was also noticeable that these high inputs of sea ice melt water in July 2014 were not confined to the shelf but were also located on the middle/end of the continental slope (Figure 5). This was also found in surface samples of a cruise further north near 53°N in late June 2014. Although this could be the signature of interannual variability, it could also be a possible transient summer feature not captured by the crossings in the other years which happened either a month or 2 weeks earlier or up to 2 months later.

Table 3. SIM and MW Fractions in % of the 10 Samples With Relatively High SIM Fractions Calculated for July 2014 and April 2015[a]

Cruise	ID	f_{MW} (%)	f_{SIM} (%)
Jul 2014	a	8	1
Jul 2014	b	8	1
Jul 2014	c	7	0
Jul 2014	d	2	2
Jul 2014	e	3	1
Jul 2014	f	2	1
Jul 2014	g	1	0
Apr 2015	x	1	1
Apr 2015	y	1	0
Apr 2015	z	1	1

[a]For reference, most negative SIM fractions are equal to −3% (S ≈ 32.25) and lowest SIM fractions around S ≈ 34 – 34.5 are around −1%.

In April 2015 (green points with a black cross in Figure 5), three samples with salinity ranging from 33.3 to 34 show high inputs of sea ice melt compared to other winter cruises, in which SIM fractions are mostly negative and can reach −0.03 (see Table 3). These samples are located to the east of Flemish cap (Figure 5), thus relatively far from the sea ice tongue at the time. These observations from April 2015 and July 2014 of strong input of SIM over the continental slope indicate a contribution of freshwater from SIM that would likely penetrate in the interior subpolar gyre [*Fratantoni and McCartney*, 2010]. Notice that these 10 samples with particularly high SIM fractions have usual MW fractions compared to nearby samples (Table 3).

4.3.2. Comparison With the Mid-1990s

Could the SURATLANT project be used to investigate the decadal variability of the LC freshwater components? Here, we present all the SURATLANT samples for which isotopic measurements were performed to compare two periods: 1994–1995 and 2012–2015. As explained previously, the mid-1990s isotopic data (LDEO) have been adjusted by −0.15‰ (see section 2.3). Both periods reveal a complex δ^{18}O-S relationship with a break slope around S = 33.65 (see figure 6). The complex mixing lines indicate that for the two periods, the surface water over the Newfoundland shelf and slope was strongly affected by sea ice processes. However, the slope break was more pronounced during the 1994–1995 period compared to the recent period. For further interpretation, we calculated the linear regressions for each period separately for salinities less than 33.65 and for salinities larger than 33.65. The results are presented in Table 4 and the linear regressions are shown in Figure 6 (black lines).

For salinities larger than 33.65, the linear regressions indicate a stronger slope and a lower *y* intercept for the 1994–1995 period (−28.08 ± 1.57) compared to the more recent period (−22.47 ± 1.54) and suggest a stronger impact of brine formation over the continental slope during the 1994–1995 period.

Over the shelf and for both periods, the slope was clearly lower than for samples with S > 33.65 and the higher *y* intercept indicated the influence of sea ice melt at the surface. The linear regressions for the two periods are not significantly different, but Figure 6 shows that 2012–2015 isotopic compositions were slightly enriched compared to the 1994–1995 period. The period 1994–1995 corresponded to the end of a

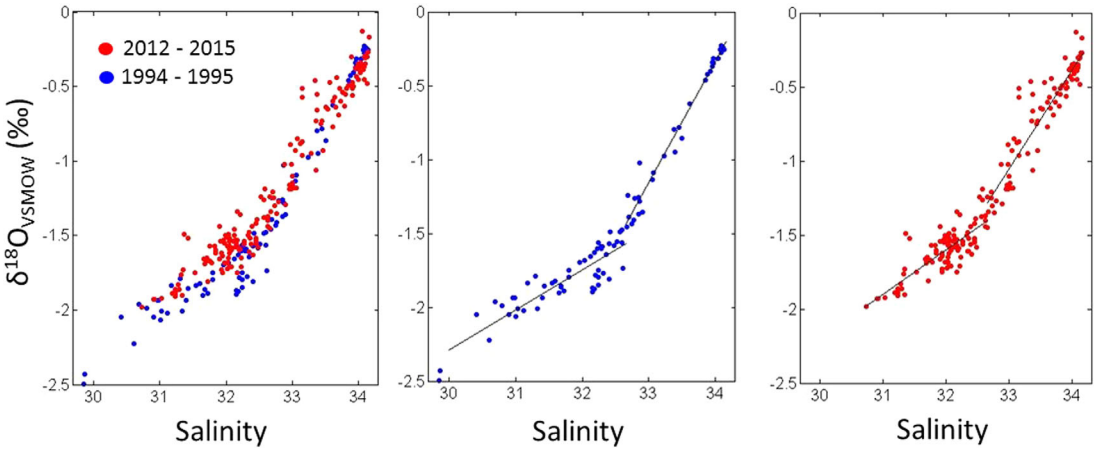

Figure 6. The δ^{18}O-S relationship in surface waters on the Newfoundland Shelf from SURATLANT measurements during two periods: 1994–1995 and 2012–2015. The 1994–1995 data (LDEO) have been corrected by −0.15‰. The δ^{18}O-S relationship is schematized by two different mixing lines for each period, with a slope break observed around S = 33.65.

Table 4. Linear Regression Equations for Salinities Less Than 33.65 (Mostly Over the Shelf) and for Salinities Larger Than 33.65 (Mostly Over the Slope)

Period	Over the Shelf ($S < 33.65$)	Over the Slope ($S > 33.65$)
1994–1995	$\delta^{18}O = 0.27 \pm 0.04$ $S - 10.48 \pm 1.24$ $R = 0.81$	$\delta^{18}O = 0.82 \pm 0.05$ $S - 28.08 \pm 1.57$ $R = 0.98$
2012–2015	$\delta^{18}O = 0.30 \pm 0.05$ $S - 11.23 \pm 1.43$ $R = 0.77$	$\delta^{18}O = 0.65 \pm 0.05$ $S - 22.47 \pm 1.54$ $R = 0.94$

period of strong positive NAO (North Atlantic Oscillation) where winters were particularly cold and the intensity of the west part of the SPG was strong, as well as the sea ice extent in the Labrador sea [e.g., *Hurrell et al*., 2003]. Note that 2014 and 2015 were also periods of strong positive NAO, but they followed a period of weaker gyre circulation and much warmer surface water (including 2012–2013). The difference in the $\delta^{18}O$-S relationship between the two periods is possibly also indicative of changes upstream in the Arctic associated with a large reduction of sea ice thickness and cover, and thus a decrease of the SIM fractions of this water advected in the Labrador Current.

5. Conclusions

This study used nutrients, oxygen isotopes, and salinity of surface sea water in the LC, to investigate the control of their variations by the seasonal variation of sea ice melt and meteoric water inputs. The amplitude of the seasonal cycle of salinity is largely explained by the variable influence of MW and SIM input, with a stronger contribution of seasonal cycle in MW input over the middle shelf (2/3 in MW and 1/3 in SIM). The largest seasonal salinity variations were observed in the Newfoundland middle shelf, with smaller variations in the inner shelf. We explain this distribution by a strong input of MW during the whole year in the inner shelf, while the MW fraction is more contrasted between summer and winter over the middle shelf. Notice that we assumed that there was no seasonal or interannual variations in the proportion of Pacific water, an assumption that needs additional work to be confirmed, but which should have little impact on SIM input, and a moderate influence on MW input estimations from our sensitivity tests. The measurements also indicate that in the summer 2014 and in April 2015, patches of large SIM contributions were located on the continental slope or further offshore, that could be potentially exported to the interior gyre. This illustrates the potential impact of sea ice melt water export in the surface LC on the stratification of the interior gyre.

With the fast changes in the Arctic Ocean and the Arctic regions such as the excess melting of the Greenland ice-sheet, the decrease of sea ice cover or the increase of arctic runoff and precipitation [e.g., *Peterson et al*., 2002; *Comiso et al*., 2008; *Shepherd et al*., 2012], the freshwater export into the North Atlantic SPG requires further attention, and more specifically the surface Labrador Current as an important pathway to bring the freshwater from the Arctic Ocean to the SPG. This study is part of a long-term measurement program SURATLANT that could be used to constrain the exchanges between the Arctic domain and the SPG on a few decades. For instance, although this study is not sufficient to attribute the changes in the distributions between the mid-1990s and the more recent period, they hint of changes that took place further upstream in the Arctic Ocean, and not just in the Labrador Sea. An ultimate goal will be to describe how the potential salinity anomalies due to the recent Arctic climate changes enter to the interior SPG and affect the winter convection.

Appendix A: Intercomparison With Different Laboratories

Here we discuss the results of inter-comparisons done between different laboratories. Five international anonymous laboratories have participated to this exercise. The aim is to evaluate the absolute precision of the isotopic measurement done at LOCEAN and to evaluate if measurements done by LS are comparable with measurements done by IRMS-Aquaprep.

First, we did three freshwater comparisons with laboratories using the same type of LS (Picarro L21-30i). We found a very good agreement with each laboratory, indicating that the absolute precision in the V-SMOW scale reached at LOCEAN is high. The results are presented in the Table A1. We did not compare sea water measurements done with LS because we did not find any laboratory performing sea water

Table A1. Results of the Freshwater Comparisons With Three Other Laboratories Using Laser Spectrometry

Laboratory	$\delta^{18}O_{LOCEAN}$	$\delta^{18}O_{Laboratory}$	Method
1	0.43	0.40	We analyzed 11 times the same sample from Jun 2013 to Jan 2014.
2	−7.36	−7.38	We exchanged six different freshwater samples with another laboratory.
	−0.77	−0.79	
	−7.18	−7.23	
	−6.61	−6.60	
	−0.05	−0.05	
	−3.26	−3.27	
3	−6.61	−6.54	We exchanged three different freshwater samples with another laboratory.
	−0.05	−0.06	
	−3.26	−3.29	

Table A2. Results of the Freshwater (FW) and Sea Water (SW) Comparisons With Two Other Laboratories Using IRMS-Aquaprep Spectrometry System

LABORATORY	Samples	$\delta^{18}O_{LOCEAN}$	$\delta^{18}O_{LABORATORY}$	Difference
4	SW	−1.14	−1.07	−0.07
4	SW	−0.19	−0.09	−0.1
4	SW	0.14	0.24	−0.1
4	SW	0.19	0.34	−0.15
4	SW	0.18	0.32	−0.14
4	SW	0.24	0.37	−0.13
4	SW	0.22	0.34	−0.12
4	SW	−0.75	−0.53	−0.22
4	SW	−0.06	0.11	−0.17
4	SW	0.17	0.43	−0.26
4	SW	0.23	0.33	−0.1
4	FW	−6.61	−6.61	0
4	FW	−3.26	−3.26	0
4	FW	−0.05	−0.06	0.01
5	SW	0.26	0.39	−0.13
5	SW	0.29	0.41	−0.12
5	SW	0.17	0.29	−0.12
5	SW	−0.06	0.08	−0.14
5	SW	−1.35	−1.19	−0.16
5	FW	−0.05	−0.02	−0.03

analyses with the needed precision. However, the tests we did at LOCEAN to validate the distillation process confirm that measurements are in agreement for samples with and without salt.

Second, we compare the LS and IRMS-Aquaprep measurements. Two laboratories have accepted to measure freshwater and seawater samples. The results are presented in the Table A2. For sea water samples, we observe an offset of approximatively $+0.14‰$ compared to the LS measurements. The close comparison found for freshwater measurements indicates that this offset of $0.14‰$ affects specifically the sea water and is not due to the different experimental protocol of calibration in the V-SMOW scale (e.g., value of the laboratory standards, how the standards are conserved). Note that an offset of $+0.15‰$ for sea-water measurements done with a IRMS coupled with Aquaprep sample preparation system has also been observed by *Lécuyer et al.* [2009], compared to freshwater samples. We chose for this paper to adjust the IRMS-Aquaprep data by $+0.15‰$.

Appendix B: Uncertainties on the Mass Balance Calculations

First, we present the potential range of variability of the end-member properties (salinity, $\delta^{18}O$, f_{PW}). At the end, we test the sensitivity to this range of variability to infer the limitation of the method.

In the mass balance calculations, we used a salinity of 4 for sea ice, as done in most similar studies [e.g., *Aagaard and Carmarck*, 1989; *Sutherland et al.*, 2009; *Bauch et al.*, 2011; *Dodd et al.*, 2012;, *Serreze et al.*, 2006]. Here, we consider a range of variations from 4 to 6 because a salinity of 2 occurs only in very old sea ice, which is very unlikely in our study area (no multiyear sea ice has been exported to the Labrador Sea between 2012 and 2014) and a salinity of 8 seems also too high for 1 year old sea ice characteristics of the studied region.

To estimate the $\delta^{18}O$ of the sea ice by using the coefficient fractionation established by *Melling and Moore* [1995], the main difficulty is to know where the sea ice has been formed. Some studies directly used the measured $\delta^{18}O$ at the surface and applied a constant offset of $2.1‰$. But this assumes that the sea ice is formed locally or that both surface waters and brines are advected together without mixing with other waters. On the southern Labrador and Newfoundland shelf, most of the sea ice is not formed locally and originates from higher latitudes. Thus, we prefer to apply the fractionation offset between liquid and solid ($+2.1‰$) on the mean $\delta^{18}O$ value of the Arctic Ocean estimated at $-1.57‰$ [*Melling and Moore*, 1995; *Ostlund and Hut*, 1984]. Thus we use a value of $0.5‰$ in the mass balance calculations. Here, we test the sensitivity to this parameter by using a range of $\delta^{18}O$ from 0 to $1‰$.

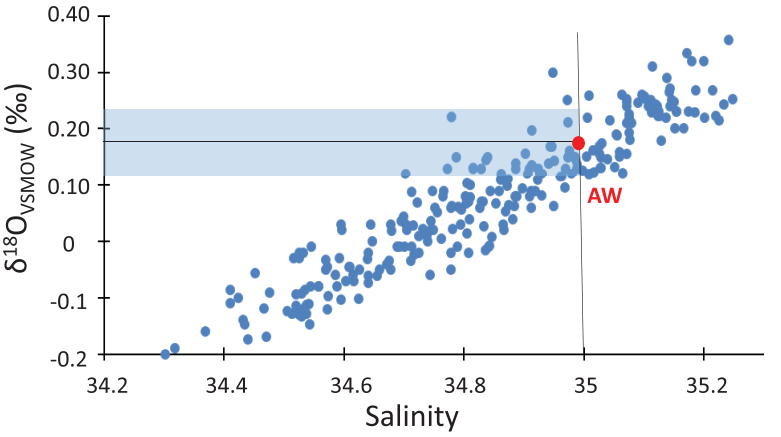

Figure B1. $\delta^{18}O$ value for the AW. ($+0.18 \pm 0.05$ ‰) for S = 35. The data are provided by the SURATLANT transect between Newfoundland and Iceland, North of 55.78 N (38.7 W).

In this study, PW is characterized by the values of S = 32.5 and $\delta^{18}O = -1‰$. We test the sensitivity of the $\delta^{18}O$-S properties with a range from 32 to 33 for salinity. In this test, salinity and $\delta^{18}O$ covary together with the relationship from *Cooper et al*. [1997].

AW is characterized by the value of S = 35 and $\delta^{18}O = +0.18‰$ from surface measurements south of Iceland provided by the full SURATLANT data set between 2012 and 2015. These samples record the AW carried by the Irminger Current. All the measurements from the transect Newfoundland-Iceland with S between 34.3 and 35.3 are presented in Figure B1. The red point indicates the AW end-member used for the mass balance calculations. Thus, we use this value in agreement with all our measurements done by laser spectrometry. Notice that the value of $+0.18‰$ is lower than the reference commonly used for AW in other previous studies [e.g., *Dodd et al*., 2012; *Sutherland et al*., 2009] ($\delta^{18}O = +0.30‰$ for S = 35/34.90). But, the value of $\delta^{18}O = +0.30‰$ has been estimated from Isotopic Ratio Mass Spectrometer measurements based on the method of equilibration between the sample and the CO_2 gas [*Epstein and Mayeda*, 1953]. The difference of 0.12‰ between these two AW end-members is close to the bias of 0.14–0.15‰, that we observed between LS and IRMS method.

Larger uncertainties exist in the $\delta^{18}O$ value of MW. Precipitation north of 60°N has values of $-21 \pm 0.7‰$, (data from the report IAEA (1981) used by *Östlund and Hut* [1984]). However, measurements during the full year over the Arctic Ocean are rare due to the difficulties of sampling. A few samples of snow show a large

Table B1. Results of Sensitivity Tests[a]

Variable	Value	fMW	fSIM	Difference (f_{MW})	Difference (f_{SIM})
S_{SI}	4	7.3	−2.8		
	6	7.3	−3.0	0.0	−0.2
$\delta^{18}O_{SI}$ (‰)	0	7.4	−2.9		
	1	7.2	−2.8	−0.2	0.2
S_{PW} and $\delta^{18}O_{PW}$ (‰)	S=32; $\delta^{18}O$=−1.3	6.7	−2.8		
	S=33; $\delta^{18}O$=−0.6	8.0	−3.1	1.3	−0.3
$\delta^{18}O_{AW}$ (‰)	0.13	7.1	−2.7		
	0.23	7.5	−3.0	0.3	−0.4
$\delta^{18}O_{MW}$ (‰)	$\delta^{18}O$=−18.4	7.3	−2.8		
	$\delta^{18}O$=−21	6.7	−2.2	−0.6	0.7
$\delta^{18}O_{MW}$ (‰)	$\delta^{18}O$=−16	8.4	−4.0		
	$\delta^{18}O$=−23	6.1	−1.5	−2.2	2.5
f_{PW}	Δf_{PW}=20%	–	–	1.0	0.5

[a]The sensitivity of the sea ice melt and meteoric water fraction calculations was tested for the possible range of variations of the sea ice (SI) salinity and isotopic composition, Pacific water (PW) salinity and isotopic composition, Atlantic water (AW) isotopic composition, meteoric water (MW), and the relative proportion of Pacific water. To test the uncertainties due to the f_{PW} value, we indicate the impact of a variation of 20% of f_{PW} on the SIM and MW fractions. Significant sensitivity of the fractions to the uncertainties is underlined. These tests have been done for different samples with similar results and are thus relevant for all SURATLANT samples.

range from $-29.9‰$ (at Fram 3, ice camp in late winter) to $-11‰$ (over the Arctic Ocean in late summer) [*Östlund and Hut*, 1984]. While the amount of precipitation over the Arctic Ocean cannot be precisely known, the area of the drainage basin of the major rivers flowing to the Arctic Ocean is 4 times larger than the Arctic Ocean area, indicating a stronger contribution of runoff to the ocean than precipitation. $\delta^{18}O$ of the river discharge to the Arctic Ocean have been recently measured by *Cooper et al.* [2008]. These measurements consider the seasonal cycle (flow rate and $\delta^{18}O$). The authors found a weighed mean value of $\delta^{18}O = -18.4‰$, in agreement with the study of *Ekwurzel et al.* [2001] and *Macdonald et al.* [1995]. In the Northern North Atlantic region, MW also contains continental glacial melt and snow melt and to date no precise estimation of the $\delta^{18}O$ value of its melt water is available. This estimation is particularly difficult because of the strong vertical inhomogeneity of $\delta^{18}O$ in the ice sheet [e.g., *Reeh et al.*, 2002] and because it is difficult to estimate which part of the ice sheet melts (probably not the part with the lowest $\delta^{18}O$ values). *Azetsu-Scott and Tan* [1997] made shipboard $\delta^{18}O$ measurements of snow and iceberg pieces varying from -20.2 to $-29.3‰$ with a mean value of $-26.5 \pm 2.8‰$. Local freshwater inputs (river runoff, precipitation, and snow) can also affect the Labrador and Newfoundland shelf, with probably more positive $\delta^{18}O$ value (estimations around $-14/-16‰$ from the Global Network of Isotopic composition of precipitations). A choice of $\delta^{18}O = -25‰$ for MW is extreme because glacial melt input to the LC is likely to be much less than precipitation and river input (higher $\delta^{18}O$). Moreover, *Mertz et al.* [1993] suggested a weak local freshwater input over the Labrador coast compared to the others sources. Thus, we chose $\delta^{18}O = -18.4‰$, but tested the sensitivity of our results to a variation from -16 to $-23‰$. However, we think that variations between -18 and $-21‰$ are more conceivable, since the largest part of the MW input is coming from the Arctic Ocean runoff, then continental glacial melt and a smaller part from local contribution.

Results from the sensitivity tests are reported in Table B1. The sea ice melt and meteoric water fraction calculations were tested for the possible range of variations of the sea ice salinity and isotopic composition, Pacific water salinity and isotopic composition, Atlantic water isotopic composition, meteoric water, and the relative proportion of Pacific water. The two last columns show the difference between fractions (MW and SIM) estimated with the reference and extreme end-members. These tests show that largest uncertainties of this method reside in the choice of (1) PW $\delta^{18}O$ and S (2) MW $\delta^{18}O$ and (3) PW fractions. These variations are conceivable and can have an effect of approximatively 1% on the MW and SIM fraction.

Acknowledgments

The surface sampling (Suratlant) is supported by INSU and SO SSS in France, and was initiated while two of the coauthors, GR and SK, were at LDEO (Columbia University, New York). The contribution of the Marine Research Institute and in particular from Hedinn Valdimarsson, Magnus Danielsen, and Alice Benoit Cattin Breton was very instrumental in the success of this long term project. Numerous ship riders have been painstakingly collecting the water samples and have always been very well received by the ship's captain and crew on Skogafoss and earlier vessels of this EIMSKIP line between Iceland and the eastern USA. We are very grateful to the companies EIMSKIP, W. Bockstiegel Maritime Service GmbH, and GRS Rohden Shipping GmbH & Co. for welcoming the ship riders. We deeply thank two anonymous reviewers for their very useful comments that improved the quality of this paper. One can access the data used to produce the results of this paper by contacting Marion Benetti (marion.benetti@locean-ipsl.upmc.fr). All the data in this project are also available at LOCEAN/IPSL (https://suratlant.locean-ipsl.upmc.fr/).

References

Aagaard, K., and E. C. Carmack (1989), The role of sea ice and other fresh water in the Arctic circulation, *J. Geophys. Res.: Oceans*, *94*(C10), 14485–14498, doi:10.1029/JC094iC10p14485.

Arrigo, K. R. (2005), Marine microorganisms and global nutrient cycles, *Nature*, *437*(7057), 349–355.

Azetsu-Scott, K., and F. C. Tan (1997), Oxygen isotope studies from Iceland to an East Greenland Fjord: Behaviour of glacial meltwater plume, *Mar. Chem.*, *56*(3), 239–251.

Bauch, D., M. R. van der Loeff, N. Andersen, S. Torres-Valdes, K. Bakker, and E. P. Abrahamsen (2011), Origin of freshwater and polynya water in the Arctic Ocean halocline in summer 2007, *Prog. Oceanogr.*, *91*(4), 482–495, doi:10.1016/j.pocean.2011.07.017.

Belkin, I. M. (2004), Propagation of the "Great Salinity Anomaly" of the 1990s around the northern North Atlantic, *Geophys. Res. Lett.*, *31*, L08306, doi:10.1029/2003GL019334.

Comiso, J. C., C. L. Parkinson, R. Gersten, and L. Stock (2008), Accelerated decline in the Arctic sea ice cover, *Geophys. Res. Lett.*, *35*, L01703, doi:10.1029/2007GL031972.

Cooper, L. W., T. E. Whitledge, J. M. Grebmeier, and T. Weingartner (1997), The nutrient, salinity, and stable oxygen isotope composition of Bering and Chukchi Seas waters in and near the Bering Strait, *J. Geophys. Res.*, *102*(C6), 12,563–12,573.

Cooper, L. W., J. W. McClelland, R. M. Holmes, P. A. Raymond, J. J. Gibson, C. K. Guay, and B. J. Peterson (2008), Flow-weighted values of runoff tracers ($\delta^{18}O$, DOC, Ba, alkalinity) from the six largest Arctic rivers, *Geophys. Res. Lett.*, *35*, L18606, doi:10.1029/2008GL035007.

Craig, H., and L. I. Gordon (1965), Deuterium and oxygen 18 variations in the ocean and the marine atmosphere, in Stable Isotopes in Oceanographic Studies and Paleo-temperatures, edited by E. Tongiorgi, pp. 91–30, CNR, Spoleto.

Desbruyères, D., H. Mercier, and V. Thierry (2015), On the mechanisms behind decadal heat content changes in the eastern subpolar gyre, *Prog. Oceanogr.*, *132*, 262–272.

Dickson, R. R., J. Meincke, S.-A. Malmberg, and A. J. Lee (1988), The "great salinity anomaly" in the Northern North Atlantic 1968–1982, *Prog. Oceanogr.*, *20*(2), 103–151, doi:10.1016/0079-6611(88)90049-3.

Dodd, P. A., B. Rabe, E. Hansen, E. Falck, A. Mackensen, E. Rohling, C. Stedmon, and S. Kristiansen (2012), The freshwater composition of the Fram Strait outflow derived from a decade of tracer measurements, *J. Geophys. Res.*, *117*, C11005, doi:10.1029/2012JC008011.

Epstein, S., and T. K. Mayeda (1953), Variations of the 18O/16O ratio in natural waters, *Geochimica et Cosmochimica Acta*, *4*(5), 213–224.

Ekwurzel, B., P. Schlosser, R. A. Mortlock, R. G. Fairbanks, and J. H. Swift (2001), River runoff, sea ice meltwater, and Pacific water distribution and mean residence times in the Arctic Ocean, *J. Geophys. Res.*, *106*(C5), 9075–9092.

Falkowski, P. G., and C. S. Davis (2004), Natural proportions, *Nature*, *431*(7005), 131–131.

Fratantoni, P. S., and M. S. McCartney (2010), Freshwater export from the Labrador Current to the North Atlantic Current at the Tail of the Grand Banks of Newfoundland, *Deep Sea Res., Part I*, *57*(2), 258–283, doi:10.1016/j.dsr.2009.11.006.

Hurrell, J. W., Y. Kushnir, G. Ottersen, and M. Visbeck (2003), *An overview of the North Atlantic oscillation, in The North Atlantic Oscillation: Climatic Significance and Environmental Impact, Geophys. Monogr.*, vol. 134, pp. 1–36, edited by J. W. Hurrell et al., AGU, Washington, D. C.

Jones, E. P., L. G. Anderson, and J. H. Swift (1998), Distribution of Atlantic and Pacific waters in the upper Arctic Ocean: Implications for circulation, *Geophys. Res. Lett.*, *25*(6), 765–768.
Jones, E. P., L. G. Anderson, S. Jutterström, L. Mintrop, and J. H. Swift (2008), Pacific freshwater, river water and sea ice meltwater across Arctic Ocean basins: Results from the 2005 Beringia Expedition, *J. Geophys. Res.*, *113*, C08012, doi:10.1029/2007JC004124.
Khatiwala, S. P., R. G. Fairbanks, and R. W. Houghton (1999), Freshwater sources to the coastal ocean off northeastern North America: Evidence from H2 18O/H2 16O , *J. Geophys. Res.*,*104*(C8), 18,241–18,255.
Latif, M., C. Böning, J. Willebrand, A. Biastoch, J. Dengg, N. Keenlyside, U. Schweckendiek, and G. Madec (2006). Is the thermohaline circulation changing?, *J. Clim.*, *19*(18), 4631–4637.
Lazier, J. R. N. (1973), The renewal of Labrador Sea water, *Deep Sea Res. Oceanogr. Abstr. 20*(4) 341–353.
Lazier, J. R. N., and D. G. Wright (1993), Annual Velocity Variations in the Labrador Current, *J. Phys. Oceanogr.*, *23*(4), 659–678, doi:10.1175/1520-0485(1993)023 < 0659:AVVITL>2.0.CO;2.
Lécuyer, C., V. Gardien, T. Rigaudier, F. Fourel, F. Martineau, and A Cros (2009), Oxygen isotope fractionation and equilibration kinetics between CO_2 and H_2O as a function of salinity of aqueous solutions, *Chem. Geol.*, *264*(1–4), 122–126, doi:10.1016/j.chemgeo.2009.02.017.
Lique, C., A. M. Treguier, B. Blanke, and N. Grima (2010), On the origins of water masses exported along both sides of Greenland: A Lagrangian model analysis, *J. Geophys. Res.*, *115*, C05019, doi:10.1029/2009JC005316.
Loder, J. W., W. C. Boicourt, and J. H. Simpson (1998), Western ocean boundary shelves coastal segment (W), *Sea*, *11*, 3–27.
Macdonald, R. W., D. W. Paten, and E. C. Carmack (1995), Based on salinity and measurements in water, *J. Geophys. Res.*, *100*(C1), 895–919.
Melling, H., and R. M. Moore (1995), Modification of halocline source waters during freezing on the Beaufort Sea shelf: Evidence from oxygen isotopes and dissolved nutrients, *Cont. Shelf Res.*, *15*(1), 89–113.
Mertz, G., S. Narayanan, and J. Helbig (1993), The freshwater transport of the Labrador current, *Atmos. Ocean*, *31*(2), 281–295, doi:10.1080/07055900.1993.9649472.
Myers, R. A., S. A. Akenhead, and K. Drinkwater (1990), The influence of Hudson Bay runoff and ice-melt on the salinity of the inner Newfoundland Shelf, *Atmos. Ocean*, *28*(2), 241–256.
Olafsson, J., S. R. Olafsdottir, A. Benoit-Cattin, and T. Takahashi (2010), The Irminger Sea and the Iceland Sea time series measurements of sea water carbon and nutrient chemistry 1983–2008, *Earth System Science Data*, *2*(1), 99–104.
Östlund, H. G., and G. Hut (1984), Arctic Ocean water mass balance from isotope data, *J. Geophys. Res.*, *89*(C4), 6373–6381.
Peterson, B. J., R. M. Holmes, J. W. McClelland, C. J. Vörösmarty, R. B. Lammers, A. I. Shiklomanov, I. A. Shiklomanov, and S. Rahmstorf (2002), Increasing river discharge to the Arctic Ocean, *Science*, *298*(5601), 2171–2173.
Rabe, B., P. A. Dodd, E. Hansen, E. Falck, U. Schauer, A. Mackensen, A. Beszczynska-Möller, G. Kattner, E. J. Rohling, and K. Cox (2013), Liquid export of Arctic freshwater components through the Fram Strait 1998–2011, *Ocean Sci.*, *9*(1), 91–109.
Redfield, A. C. (1958), The biological control of chemical factors in the environment, *American scientist*, *46*(3), 230A–221.
Redfield, A. C. (1963), The influence of organisms on the composition of sea-water, *The sea*, 26–77.
Reeh, N., H. Oerter, and H. H. Thomsen (2002), Comparison between Greenland ice-margin and ice-core oxygen-18 records, *Ann. Glaciol.*, *35*(1), 136–144, doi:10.3189/172756402781817365.
Reverdin, G., P. P. Niiler, and H. Valdimarsson (2003), North Atlantic Ocean surface currents, *J. Geophys. Res.*, *108*(C1), 3002, doi:10.1029/2001JC001020.
Reverdin, G. (2010), North Atlantic subpolar gyre surface variability (1895–2009), *J. Clim.*, *23*(17), 4571–4584, doi:10.1175/2010JCLI3493.1.
Rhein, M., J. Fischer, W. M. Smethie, D. Smythe-Wright, R. F. Weiss, C. Mertens, D.-H. Min, U. Fleischmann, and A. Putzka (2002), Labrador Sea Water: Pathways, CFC inventory, and formation rates, *J. Phys. Oceanogr.*, *32*(2), 648–665.
Serreze, M. C., et al. (2006), The large-scale freshwater cycle of the Arctic, *J. Geophys. Res.: Oceans*, *111*(C11).
Shepherd, A., et al. (2012), A reconciled estimate of ice-sheet mass balance, *Science*, *338*(6111), 1183–1189.
Skrzypek, G., and D. Ford (2014), Stable Isotope analysis of saline water samples on a cavity ring-down spectroscopy instrument, *Environ. Sci. Technol.*, *48*(5), 2827–2834, doi:10.1021/es4049412.
Steur, L., R. S. Pickart, D. J. Torres, and H. Valdimarsson (2015), Recent changes in the freshwater composition east of Greenland, *Geophys. Res. Lett.*, *42*, 2326–2332, doi:10.1002/2014GL062759.
Straneo, F., and F. Saucier (2008), The outflow from Hudson Strait and its contribution to the Labrador Current, *Deep Sea Res., Part I*, *55*(8), 926–946, doi:10.1016/j.dsr.2008.03.012.
Sutherland, D. A., R. S. Pickart, E. Peter Jones, K. Azetsu-Scott, A. Jane Eert, and J. Ólafsson (2009), Freshwater composition of the waters off southeast Greenland and their link to the Arctic Ocean, *J. Geophys. Res.*, *114*, C05020, doi:10.1029/2008JC004808.
Taylor, J. R., K. K. Falkner, U. Schauer, and M. Meredith (2003), Quantitative considerations of dissolved barium as a tracer in the Arctic Ocean, *J. Geophys. Res.*, *108*(C12), 3374, doi:10.1029/2002JC001635.
Yamamoto-Kawai, M., F. A. McLaughlin, E. C. Carmack, S. Nishino, and K. Shimada (2008), Freshwater budget of the Canada Basin, Arctic Ocean, from salinity, δ^{18}O, and nutrients, *J. Geophys. Res.*, *113*, C01007, doi:10.1029/2006JC003858.
Yashayaev, I., and J. W. Loder (2009), Enhanced production of Labrador Sea water in 2008, *Geophys. Res. Lett.*, *36*, L01606, doi:10.1029/2008GL036162.
Yashayaev, I., H. M. van Aken, N. P. Holliday, and M. Bersch (2007), Transformation of the Labrador sea water in the subpolar North Atlantic, *Geophys. Res. Lett.*, *34*, L22605, doi:10.1029/2007GL031812.
Woodgate, R. A., and K. Aagaard (2005), Revising the Bering Strait freshwater flux into the Arctic Ocean, *Geophys. Res. Lett.*, *32*, L02602, doi:10.1029/2004GL021747.